Exploration of jet substructure using iterative declustering in pp and Pb–Pb collisions at LHC energies

ALICE Collaboration; Acharya, S.; Andrews, H.A.; Evans, David; Graham, K.L.; Jevons, O.; Jones, P.G.; Jusko, A.; Krivda, M.; Kvapil, J.; Lietava, R.; Ragoni, S.; Villalobos Baillie, O.; Willsher, E.; Zardoshti, N.

Link to publication on Research at Birmingham portal

Exploration of jet substructure using iterative declustering in pp and Pb–Pb collisions at LHC energies

ALICE Collaboration[⋆]

ABSTRACT

The ALICE collaboration at the CERN LHC reports novel measurements of jet substructure in pp collisions at $\sqrt{s} = 7$ TeV and central Pb–Pb collisions at $\sqrt{s_{NN}} = 2.76$ TeV. Jet substructure of track-based jets is explored via iterative declustering and grooming techniques. We present the measurement of the momentum sharing of two-prong substructure exposed via grooming, the z_g, and its dependence on the opening angle, in both pp and Pb–Pb collisions. We also present the measurement of the distribution of the number of branches obtained in the iterative declustering of the jet, which is interpreted as the number of its hard splittings. In Pb–Pb collisions, we observe a suppression of symmetric splittings at large opening angles and an enhancement of splittings at small opening angles relative to pp collisions, with no significant modification of the number of splittings. The results are compared to predictions from various Monte Carlo event generators to test the role of important concepts in the evolution of the jet in the medium such as colour coherence.

© 2020 The Author(s). Published by Elsevier B.V. This is an open access article under the CC BY license (http://creativecommons.org/licenses/by/4.0/). Funded by SCOAP³.

1. Introduction

The objective of the heavy-ion jet physics program at the LHC is to probe fundamental, microscopic properties of nuclear matter at high densities and temperatures. Jets provide well-calibrated probes of the dense medium created in heavy-ion collisions. In pp collisions, the production of jets and their substructure have been measured extensively and these measurements are well-reproduced by theoretical calculations based on perturbative QCD (pQCD) (see Refs. [1–4] and citations therein). Jets are produced in high-momentum transfer processes, which occur on time scales much shorter than the formation time of the Quark-Gluon Plasma (QGP) generated in heavy-ion collisions; the production rates of jets in heavy-ion collisions can therefore be calculated accurately using the same pQCD approaches as for pp collisions, after taking into account the effects of nuclear geometry and nuclear modification of parton distribution functions (PDFs) [5].

Jets traversing the QGP will interact via elastic and radiative processes which modify the reconstructed jet cross section and structure relative to jets in vacuum ("jet quenching") [6]. Jet quenching effects have been extensively observed in nuclear collisions at RHIC and LHC in measurements of inclusive production and correlations of high-p_T hadrons and jets, including correlations of high-energy triggers (hadrons, photons, W and Z bosons, and jets) and reconstructed jets [7–10] as well as in the measure-

ment of jet shapes [11–16]. Comparisons of these measurements to theoretical jet quenching calculations enable the determination of dynamical properties of the QGP, notably the transport parameter $\hat{q}$ [17].

More recently, the modification of the jet substructure due to jet quenching has been explored in heavy-ion collisions using tools developed for the measurement of jet substructure in pp collisions for QCD studies and Beyond Standard Model searches [2,18]. A key tool is iterative declustering, which subdivides jets into branches or splittings that can be projected onto the phase space of such splittings, called the Lund plane [19–21]. While the splitting map contains kinematic information of all splittings, techniques like grooming [22,23] can be applied to isolate a specific region of the splitting map according to different criteria such as mitigation of non-perturbative effects, enhancement of the jet quenching signal or simplification of perturbative calculations.

In this work we focus on the Mass Drop [22] or Soft Drop (SD) grooming [23] with $z_{cut} = 0.1$ and $\beta = 0$. This technique selects the first splitting in the declustering process for which the subleading prong carries a fraction z of the momentum of the emitting prong larger than z_{cut}. Note that this criterion selects a subset of the splittings. The grooming procedure removes soft radiation at large angles to expose a two-prong structure in the jet. The shared momentum fraction of those prongs is called z_g, the groomed subjet momentum balance. The measurement of z_g in vacuum is closely related to the Altarelli-Parisi splitting functions [23].

⋆ *E-mail address:* alice-publications@cern.ch.

Theoretical considerations of the in-medium modification of z_g can be found in [24–27]. A key physics ingredient in the theoretical calculations is colour coherence [28]. This is the effect by which a colour dipole cannot be resolved by the medium as two independent colour charges if the opening angle of the dipole is small compared to a fundamental medium scale. If the dipole cannot be resolved, it will propagate through the medium as a single colour charge. If colour coherence is at work, there will be parts of the jet substructure that won't be resolved, leading to a reduced effective number of colour charges and thus a reduced amount of energy loss in medium.

With the grooming technique we select a hard two-prong substructure. Then we inspect the dependence on the opening angle of the rate of such two-prong objects in medium relative to vacuum. We are interested in understanding whether large-angle splittings are more suppressed relative to vacuum than small-angle splittings, as one would expect if large-angle splittings are resolved by the medium and radiate in the medium incoherently. Previous measurements of z_g by the CMS collaboration [29] show a modification in central Pb–Pb collisions relative to the pp reference whilst measurements performed at RHIC by the STAR collaboration showed no modification [30]. Those measurements did not scan the ΔR dependence and cover different intervals of the subleading prong energies that can bias towards different typical splitting formation times.

This work reports the measurement by the ALICE collaboration of z_g, the shared momentum fraction of two-prong substructure, its dependence on the opening angle and n_{SD}, the number of splittings satisfying the grooming condition obtained via the iterative declustering of the jet [31], in pp collisions at $\sqrt{s} = 7$ TeV and central (0–10%) Pb–Pb collisions at $\sqrt{s_{NN}} = 2.76$ TeV.

2. Data sets and event selection

A detailed description of the ALICE detector and its performance can be found in Refs. [32,33]. The analysed pp data were collected during Run 1 of the LHC in 2010 with a collision centre-of-mass energy of $\sqrt{s} = 7$ TeV using a minimum bias (MB) trigger. The MB trigger configuration is the same as described in Ref. [34]. The data from heavy-ion collisions were recorded in 2011 at $\sqrt{s_{NN}} = 2.76$ TeV. This analysis uses the 0–10% most-central Pb–Pb collisions selected by the online trigger based on the hit multiplicity measured in the forward V0 detectors [35]. The datasets and event selection are identical to Refs. [7,11]. After offline selection, the pp sample consists of 168 million events, while the Pb–Pb sample consists of 19 million events.

The analysis uses charged tracks reconstructed by the Inner Tracking System (ITS) [36] and Time Projection Chamber (TPC) [37] which both cover the full azimuth and pseudo-rapidity $|\eta| < 0.9$. Tracks are required to have transverse momentum $0.15 < p_T < 100$ GeV/c. The track selection is slightly different in the analysis of the 2010 and the 2011 data. The former uses a subclass of tracks with worse momentum resolution that is excluded from the latter [38].

In pp collisions, the tracking efficiency is approximately 80% for tracks with $p_T > 1$ GeV/c, decreasing to roughly 56% at $p_T = 0.15$ GeV/c, with a track momentum resolution of 1% for $p_T = 1$ GeV/c and 4.1% for $p_T = 40$ GeV/c [33,34,39]. In Pb–Pb collisions, the tracking efficiency is about 2 to 3% worse than in pp. The track p_T resolution is about 1% at $p_T = 1$ GeV/c and 2.5% for $p_T = 40$ GeV/c.

As a vacuum reference for the Pb–Pb measurements we use simulated pp collisions at $\sqrt{s} = 2.76$ TeV, calculated using PYTHIA 6.425 (Perugia Tune 2011) [27] and embedded into real central Pb–Pb events at the detector level, to take into account the smearing by the background fluctuations. We use the embedding of PYTHIA-generated events instead of the embedding of real pp data measured at $\sqrt{s} = 2.76$ TeV due to the limited size of the data sample. The PYTHIA MC describes well vacuum intrajet distributions [2]. In this paper, we validate the PYTHIA calculation by comparing it to jet substructure measurements in pp collisions at $\sqrt{s} = 7$ TeV.

3. Jet reconstruction

Jets are reconstructed from charged tracks using the anti-k_T algorithm [40] implemented in FastJet [41] with a jet resolution parameter of $R = 0.4$. The four-momenta of tracks are combined using the E-scheme recombination [41] where the pion mass is assumed for all reconstructed tracks. In order to ensure that all jet candidates are fully contained within the fiducial volume of the ALICE detector system, accepted jets were required to have their centroid constrained to $|\eta_{jet}| < 0.5$.

The jet finding efficiency is 100% in the measured kinematic ranges. The jet energy instrumental resolution is similar for pp and Pb–Pb collisions, varying from 15% at $p_{T,jet}^{ch} = 20$ GeV/c to 25% at $p_{T,jet}^{ch} = 100$ GeV/c. The Jet Energy Scale (JES) uncertainty is dominated by the tracking efficiency uncertainty which is 4%.

In pp collisions, no correction for the underlying event is applied. In Pb–Pb collisions, the jet energy is partially adjusted for the effects of uncorrelated background using the constituent subtraction method [42]. Constituent subtraction corrects individual jet constituents by modifying their four-momentum. The momentum that is subtracted from the constituents is determined using the underlying event density, ρ, which is calculated by clustering the event into $R = 0.2$ jets using the k_T algorithm [43,44] and taking the median jet p_T density in the event. The two leading k_T jets are removed before calculating the median, to suppress the contribution of true hard jets in the background estimation. The correction is applied such that the total momentum removed from the jet is equal to $\rho \times A_j$, where A_j is the jet area. This background subtraction is applied both to the measured data and to the embedded PYTHIA reference.

4. Observables

Jet constituents are reclustered using the physical Cambridge/Aachen (CA) metric [45], leading to an angle-ordered shower. The declustering process consists of unwinding the clustering history step by step, always following the hardest branch. The first declustering step identifies the final subjet pair or branch that was merged. The second declustering step identifies the subjet pair that was merged into the leading subjet of the final step, etc. The coordinates of the subleading prong in the Lund Plane ($\log(z\Delta R)$, $\log(1/\Delta R)$) are registered at each declustering step, where z is the fraction of momentum carried by the subleading prong $z = \frac{\min(p_{T,1}, p_{T,2})}{p_{T,1} + p_{T,2}}$, with $p_{T,1}$ and $p_{T,2}$ being the momenta of the leading and subleading prongs, respectively, and ΔR the opening angle of the splitting.

The observable n_{SD} is obtained by counting the number of splittings in the declustering process that satisfy the Soft Drop selection $z > z_{cut}$, $z_{cut} = 0.1$. The observable z_g corresponds to the subjet momentum balance, z, of the first splitting satisfying the SD selection. Jets with $n_{SD} = 0$ are labelled "untagged jets". The z_g distribution is absolutely normalised, including the untagged jets in the normalisation. This choice of normalisation, used here for the first time, provides crucial information for quantitative comparison of jet substructure measurements in Pb–Pb and pp collisions since it allows the results to be interpreted in terms of not only a change of shape in the distribution but also in terms of net enhancement/suppression of the yield of splittings satisfying the SD condition in a given jet transverse momentum range.

The tracking system enables the measurement of subjets with angular separation smaller than 0.1 radians and a scan of the z_g distribution in ranges of ΔR: $\Delta R < 0.1$, $\Delta R > 0.1$ and $\Delta R > 0.2$.

For data from pp collisions, the correction of the detector effects was performed via unfolding. The results are presented in the jet momentum interval of $40 < p_{T,jet}^{ch} < 60$ GeV/c, chosen to balance statistical precision and detector effects. In Pb–Pb collisions, the results are presented at detector-level, with the uncorrelated background subtracted on average from the jet p_T and from the substructure observable. The vacuum reference is thus smeared by background fluctuations and instrumental effects. The Pb–Pb results are presented in the jet momentum range of $80 < p_{T,jet}^{ch} < 120$ GeV/c, where uncorrelated background is negligible.

5. Corrections and systematic uncertainties

For data from pp collisions, the unfolding of instrumental effects is carried out using a four-dimensional response matrix that encodes the smearing of both jet p_T^{ch} and the substructure observable (shape^{part,ch}, $p_{T,jet}^{part,ch}$, shape^{det,ch}, $p_{T,jet}^{det,ch}$), where "shape" denotes either z_g or n_{SD}. The upper index "part" refers to particle-level and "det" refers to detector-level quantities, obtained from simulations in which pp collisions are generated by PYTHIA (particle-level) and then passed through a GEANT3-based model [46] of the ALICE detector. We note that the particle-level jet finding is performed using the true particle masses so the unfolding corrects for the pion mass assumption at detector level.

To generate vacuum reference distributions for comparison to Pb–Pb results, which are not fully corrected, we superimpose detector-level PYTHIA events onto real Pb–Pb events. Consequently, no two-track effects are present, however their impact in data is negligible due to the large required number of clusters per track. The matching of particle-level and embedded jets is performed as described in [11]. The matching efficiency is consistent with unity for jets with p_T above 30 GeV/c.

For pp collisions, Bayesian unfolding in two dimensions as implemented in the RooUnfold package [47] is used. The prior is the two-dimensional distribution ($p_{T,jet}^{part,ch}$, shape^{part,ch}) generated with PYTHIA. The default number of iterations chosen for z_g and n_{SD} is 4, which corresponds to the first iteration for which the refolded distributions agree with the corresponding raw distributions within 5%. A closure test was also carried out, in which two statistically independent Monte Carlo (MC) samples are used to fill the response and the pseudo-data. For this test, the unfolded solution agrees with the MC truth distribution within statistical uncertainties.

Unfolding of the distributions was attempted for the Pb–Pb case, but no convergence on a mathematically consistent solution was obtained, due to the limited statistics of the data sample and due to the fact that the response is strongly non-diagonal due to the presence of sub-leading prongs at large angles that are not correlated to particle-level prongs and that arise due to fluctuations of the uncorrelated background. Strategies to suppress such secondary prongs are beyond the scope of this analysis.

The systematic uncertainties are determined by varying key aspects of the correction procedures for instrumental response and background fluctuations. The most significant components of the systematic uncertainties for z_g and n_{SD} are tabulated in Table 1 and 2. For pp collisions, the tracking efficiency uncertainty is $\pm 4\%$ [15]. The effect of this uncertainty on the substructure measurement is assessed by applying an additional track rejection of 4% at detector-level prior to jet finding. A new response is built and the unfolding is repeated, with the resulting variation in the unfolded solution symmetrised and taken as the systematic uncertainty. This

is the largest contribution to the JES uncertainty. To estimate the regularisation uncertainty, the number of Bayesian iterations is varied by ± 1 with respect to the default analysis value. The prior is varied by reweighting the response such that its particle-level projection (PYTHIA) matches HERWIG 7.1.2 [48]. The detector-level intervals in p_T and the substructure observables are modified to determine what in the table is referred to as truncation uncertainty. The uncertainty labelled "Binning" in the tables corresponds to a variation in binning of both p_T and substructure observables, subject to the constraint of at least 10 counts in the least populous bin to ensure the stability of the unfolding procedure.

In the case of Pb–Pb collisions, the evaluation of the uncertainty due to tracking efficiency is carried out similarly to the pp case. The z_g measurement is done differentially in ranges of ΔR. The limits of the ΔR ranges were varied by $\pm 10\%$, which corresponds approximately to the width of the distribution of the relative difference of particle-level and embedded-level ΔR in Pb–Pb collisions. The differences between PYTHIA and the unfolded pp distributions are taken into account when using PYTHIA as a reference for Pb–Pb measurements. This is done by reweighting the embedded PYTHIA reference so that its particle-level projection matches the unfolded pp $p_{T,jet}$ vs z_g (or $p_{T,jet}$ vs n_{SD}) correlation. The difference between the reference smeared with the default and the reweighted response is assigned as the corresponding uncertainty.

In both the pp and Pb–Pb analyses, the uncertainties are added in quadrature. All the contributions to the overall uncertainty produce changes in a given interval of the distribution that are strongly anti-correlated with changes in a different interval, i.e., they induce changes in the shape of the observable.

6. Results

Figs. 1 and 2 show fully corrected distributions of z_g and n_{SD} measured in pp collisions at $\sqrt{s} = 7$ TeV for charged jets in the interval $40 < p_{T,jet}^{ch} < 60$ GeV/c. The results are compared to distributions obtained from PYTHIA 6 (Perugia Tune 2011), from PYTHIA 6 + POWHEG [49], to consider the impact of NLO effects, and from the newer PYTHIA 8 (Tune 4C) [50].

The z_g distribution is well-described within systematic and statistical uncertainties by all the MC generators considered. As discussed above, untagged jets contribute to the normalisation of the distributions. The untagged contribution is not shown in Fig. 1, due to the suppressed zero on the horizontal axis, but is shown in Fig. 2 in the bin representing $n_{SD} = 0$. Table 3 shows the tagged fraction for data and simulations. For pp (rightmost column), the untagged fraction is about 2%. The Monte Carlo distributions in Fig. 2 disagree with the data in the tails of the distribution. They have a significantly lower fraction of jets with no splittings ($n_{SD} = 0$) than observed in data. The addition of POWHEG corrections to PYTHIA 6 induces a small shift of the distribution towards a larger number of splittings.

Fig. 3 shows z_g distributions measured in central Pb–Pb collisions for various ranges of angular separation ΔR. The results are presented in the uncorrected transverse momentum range $80 \leq p_{T,jet}^{ch} < 120$ GeV/c and compared to the distribution of PYTHIA jets embedded into real 0–10% central Pb–Pb events.

Fig. 3 shows a larger difference between the measured Pb–Pb and embedded reference distributions for larger values of ΔR, indicating a relative suppression in the rate of symmetric splittings ($z_g \approx 0.5$) in central Pb–Pb collisions. However, due to the steeply falling z_g distribution, the fraction of all jets that exhibit symmetric splittings is small, and this strong suppression corresponds to a suppression of only a few percent in the total rate of jets passing

Table 1

Relative systematic uncertainties on the measured distributions in pp collisions for three selected jet shape intervals in the jet $p_{\mathrm{T,jet}}^{\mathrm{ch}}$ interval of 40–60 GeV/c. Due to the shape of the n_{SD} distribution, the systematic variations lead to a crossing at central values which artificially reduces the evaluated systematic uncertainty. To improve this we smooth the total systematic uncertainty by interpolating between neighbouring bins.

Observable	z_{g}			n_{SD}		
Interval	0.1–0.175	0.25–0.325	0.4–0.5	0	3	6
Tracking efficiency (%)	1.9	0.2	1.0	16.1	1.1	18.3
Prior (%)	$+0.0$ -3.9	$+7.6$ -0.0	$+0.0$ -9.4	$+0.0$ -1.6	$+0.0$ -9.2	$+0.0$ -21.3
Regularisation (%)	$+0.8$ -0.5	$+0.2$ -0.2	$+0.4$ -0.5	$+0.4$ -1.4	$+1.4$ -1.1	$+1.7$ -3.0
Truncation (%)	$+2.2$ -0.0	$+1.8$ -0.0	$+2.4$ -0.0	$+0.0$ -0.0	$+0.0$ -0.1	$+4.4$ -0.0
Binning (%)	0.5	4.5	1.2	N/A	N/A	N/A
Total (%)	$+3.0$ -4.4	$+8.2$ -3.0	$+2.6$ -9.6	$+16.1$ -16.2	$+7.8$ -6.2	$+18.9$ -28.2

Table 2

Relative systematic uncertainties on the measured distributions in Pb–Pb collisions for three selected jet shape intervals and one ΔR selection in the jet $p_{\mathrm{T,jet}}^{\mathrm{ch}}$ interval of 80–120 GeV/c.

Observable	$z_{\mathrm{g}}(\Delta R > 0.1)$			n_{SD}		
Interval	0.1–0.175	0.25–0.325	0.4–0.5	0	3	6
Tracking efficiency (%)	4.9	2.8	11.4	11.2	7.9	11.1
Angular cutoff (%)	$+2.3$ -3.8	$+2.8$ -0.0	$+10.0$ -0.0	N/A	N/A	N/A
Reference (%)	$+0.0$ -0.0	$+12.4$ -0.0	$+10.1$ -0.0	$+30.1$ -0.0	$+0.0$ -5.2	$+5.3$ -0.0
Total (%)	$+5.4$ -6.2	$+13.1$ -2.8	$+18.2$ -11.4	$+32.1$ -11.2	$+7.9$ -9.5	$+12.3$ -11.1
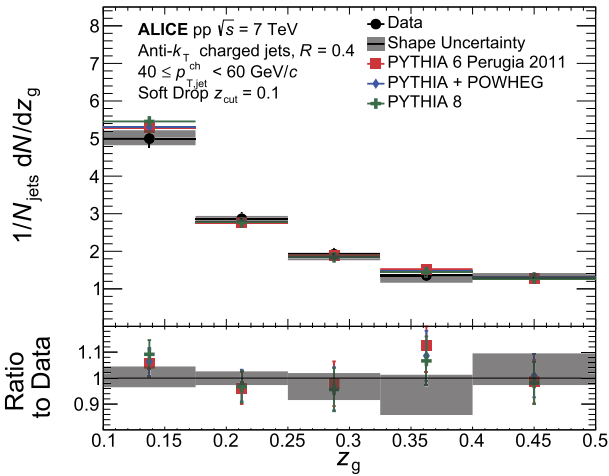
Fig. 1. Fully corrected z_{g} distribution in pp collisions for $40 \leq p_{\mathrm{T,jet}}^{\mathrm{ch}} < 60$ GeV/c compared with predictions from PYTHIA simulations. The statistical uncertainties are shown as vertical bars and the systematic uncertainties are represented by a shaded area.

Fig. 2. Fully corrected n_{SD} distribution in pp collisions for $40 \leq p_{\mathrm{T,jet}}^{\mathrm{ch}} < 60$ GeV/c, compared with predictions from PYTHIA simulations. The statistical uncertainties are shown as vertical bars and the systematic uncertainties are represented by a shaded area.

both the SD and angular cuts (cf. Table 3). Conversely, in the small ΔR limit a small excess of splittings is observed in the data.

Fig. 3 also shows comparisons to predictions from the JEWEL event generator [51] and Hybrid model [52] calculations. The JEWEL simulations include the medium response from jet-medium interactions [53]. The theoretical predictions must be smeared to account for the detector effects as well as fluctuations due to uncorrelated background. This smearing is performed by constructing a 6-dimensional response matrix by superimposing PYTHIA events at detector level to real 0–10% central Pb–Pb events. The 6-dimensional matrix maps every embedded jet from a given bin of $(z_{\mathrm{g}}^{\mathrm{part}}, \Delta R^{\mathrm{part}}, p_{\mathrm{T,jet}}^{\mathrm{part}})$ to $(z_{\mathrm{g}}^{\mathrm{det}}, \Delta R^{\mathrm{det}}, p_{\mathrm{T,jet}}^{\mathrm{det}})$. The smearing of the distributions significantly modifies the predictions and is essential for quantitative comparison of the measurements and calculations.

The models capture the qualitative trends of the data, namely the enhancement of the number of small-angle splittings and the
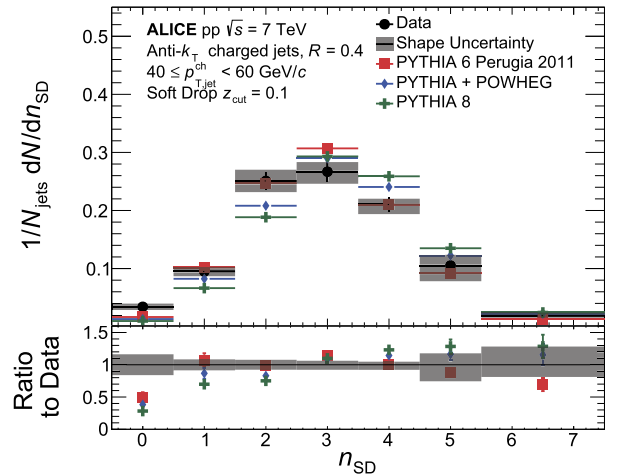
suppression of the large-angle symmetric splittings. The fraction of jets not passing the SD selection is similar in the models and data. However discrepancies are observed in the angular selection. For instance the number of SD splittings that pass the angular cut of $\Delta R > 0.2$ is the lowest in the case of the Hybrid model, pointing to a stronger incoherent quenching of the prongs.

The suppression of splittings at large opening angles is qualitatively expected from vacuum formation time and colour coherence arguments [26]. The wider the opening angle, the shorter the formation time of the splitting. This makes it more likely that the splitting propagates through, and is modified by, the medium. If coherence effects are at play in the medium then it is expected that splittings that are separated by more than the coherence angle will be more suppressed since they radiate energy independently.

Fig. 4 shows the comparison of n_{SD} distributions from Pb–Pb measurements and the embedded PYTHIA reference. The data ex-

Table 3
Fraction of jets that pass the Soft Drop condition $z_{cut} = 0.1$ in the specified range of angular separation and in the transverse momentum range $40 \leq p_{T,jet}^{ch} < 60$ GeV/c for pp and $80 \leq p_{T,jet}^{ch} < 120$ GeV/c for Pb–Pb collisions. Uncertainties on the data are written as statistical (systematic).

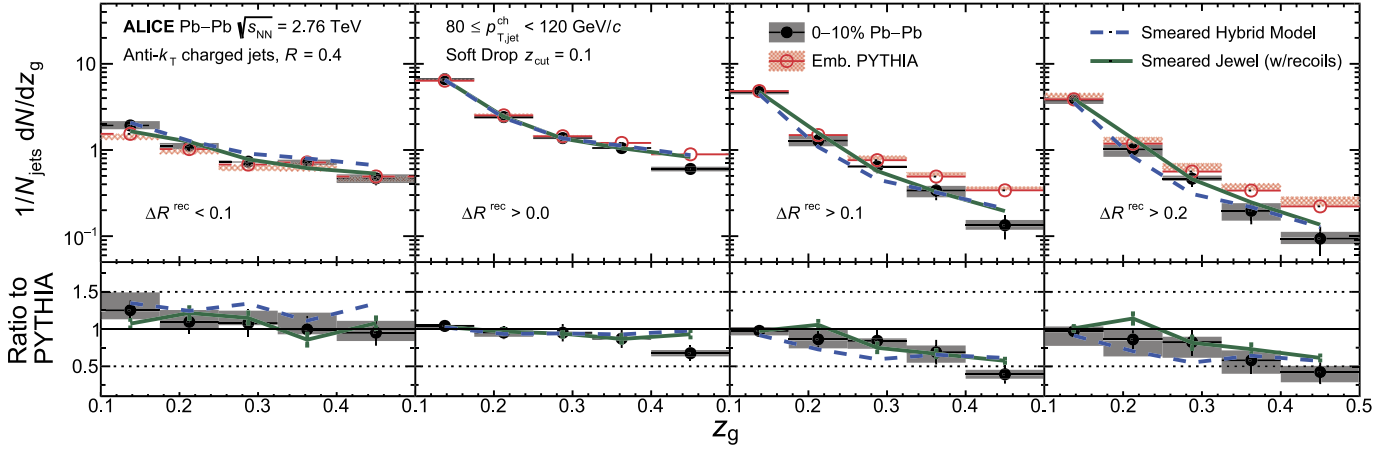| Dataset	Tagged rate (%)				
	Pb–Pb				pp
Angular Cut	$\Delta R < 0.1$	$\Delta R > 0.0$	$\Delta R > 0.1$	$\Delta R > 0.2$	$\Delta R > 0.0$
Data	$38.4 \pm 2.3(2.5)$	$92.1 \pm 3.5(0.9)$	$53.6 \pm 2.7(3.4)$	$41.8 \pm 2.4(3.6)$	$97.3 \pm 3.0(1.7)$
PYTHIA	34.6	95.5	60.2	46.9	98.6
Hybrid	47.5	93.4	45.8	35.0	N/A
JEWEL	42.0	93.0	51.0	40.0	N/A

Fig. 3. Detector-level Pb–Pb distributions of z_g for $R = 0.4$ jets with varying minimum/maximum angular separation of subjets (ΔR) for jets in the range $80 \leq p_{T,jet}^{ch} < 120$ GeV/c. The systematic uncertainties are represented by the shaded area. The corresponding values for the embedded PYTHIA reference (open symbols), Hybrid model (dashed line) and JEWEL (solid line) are also shown in the plot. The lower plots show the ratios of data, Hybrid and JEWEL model to the embedded PYTHIA reference.

hibit a shift towards lower number of splittings. The discrepancies between the distributions from PYTHIA and from pp collisions are incorporated as a part of the reference uncertainty via the reweighting procedure described above. The corresponding curves for the Hybrid model and JEWEL are also shown in the plot.

To explore the dependence of the n_{SD} distribution on the fragmentation pattern, we also show a calculation in which the pp reference distribution is based solely on light-quark fragmentation. Since the quark fragmentation is harder, we see that the number of splittings peaks at lower values, in line with what we observe in the data. The smeared JEWEL and Hybrid model calculation agree with the qualitative trend of the data.

The trends indicate that the larger the opening angle, the more suppressed the splittings are, and this is qualitatively consistent with large-angle prongs being more resolved by the medium and thus more suppressed. The same process could lead to a reduction in the number of hard splittings as observed in Fig. 4. However, it is worth noting that both the Hybrid and JEWEL models, in spite of their capturing of the general trends of the data, they do not incorporate the physics of colour coherence and all the prongs in the jet lose energy incoherently. This points to a simpler interpretation of the results for instance in terms of formation times of the splittings and their interplay with the medium length. The vacuum formation time $t_f \approx \omega/k_T^2 \approx 1/(\omega \Delta R^2)$, with ω and k_T being the energy and relative transverse momentum of the radiated prong, is shorter for large-angle splittings, meaning that vacuum, large-angle splittings, will be produced mostly in the medium and their resulting prongs will be further modified by the medium. At large angles, the component of vacuum splittings that propagate in vacuum is less than at small angles, resulting in an enhanced contribution of medium-modifications compared to small-angle splittings.
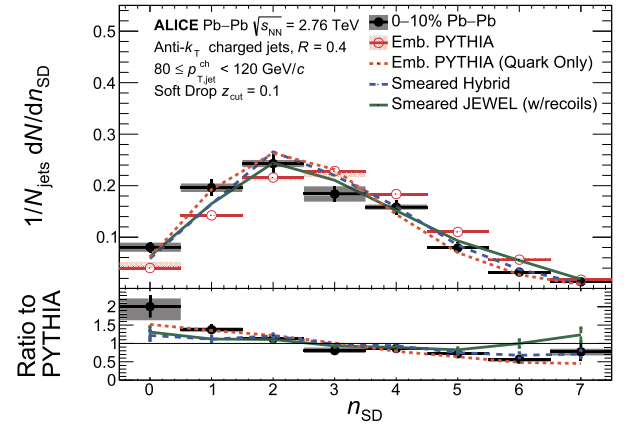

Fig. 4. The number of SD branches for jets reconstructed in Pb–Pb data are shown. The systematic uncertainties are represented by the shaded area. The datapoints are compared to jets found in PYTHIA events embedded into Pb–Pb events (open markers). The Hybrid model and JEWEL predictions correspond to the red (dashed) and blue (solid) lines. The lower panel shows the ratio of the n_{SD} distribution in data and the embedded PYTHIA reference (grey). The ratios of the Hybrid and JEWEL models to the embedded PYTHIA reference are also shown and their uncertainties are purely statistical.

7. Summary

This Letter presents the measurement of jet substructure using iterative declustering techniques in pp and Pb–Pb collisions at the LHC. We report distributions of n_{SD}, the number of branches passing the soft drop selection, and z_g, the shared momentum fraction of the two-prong substructure selected by the mass drop condition, differentially in ranges of splitting opening angle.

Generally, good agreement between distributions for pp collisions and vacuum calculations is found except for the fraction of untagged jets, which is underestimated by the models. In Pb–Pb collisions, a suppression of the z_g distribution is observed at large angles relative to the vacuum reference whilst at low opening angles there is a hint of an enhancement. These observations are in qualitative agreement with the expected behaviour of two-prong objects in the case of coherent or decoherent energy loss [26] in the BMDPS-Z [54,55] framework. However, the models that are compared to the data do not implement colour coherence and yet they capture the qualitative trends of the data. This suggests that other effects might drive the observed behaviour, for instance the interplay between formation time of the splittings and medium length.

The number of splittings obtained by iteratively declustering the hardest branch in the jet, n_{SD}, is shifted towards lower values in Pb–Pb relative to the vacuum reference. This suggests that medium-induced radiation does not create new splittings that pass the SD cut. On the contrary, there is a hint of fewer splittings passing the SD cut, pointing to a harder, more quark-like fragmentation in Pb–Pb compared to pp collisions, in qualitative agreement with the trends observed for other jet shapes [11].

With these measurements, we have explored a region of the Lund plane delimited by the Soft Drop cut $z > 0.1$. Other regions of the phase space of splittings will be scanned systematically in the future with larger data samples.

Acknowledgements

References

[1] M. Dasgupta, F.A. Dreyer, G.P. Salam, G. Soyez, Inclusive jet spectrum for small-radius jets, J. High Energy Phys. 06 (2016).

[2] L. Asquith, et al., Jet Substructure at the Large Hadron Collider: Experimental Review.

[3] CMS Collaboration, A.M. Sirunyan, et al., Measurement of jet substructure observables in $t\bar{t}$ events from proton-proton collisions at $\sqrt{s} = 13$ TeV, Phys. Rev. D 98 (9) (2018), arXiv:1808.07340 [hep-ex].

[4] A.J. Larkoski, I. Moult, B. Nachman, Jet substructure at the large hadron collider: a review of recent advances in theory and machine learning, arXiv:1709.04464 [hep-ph].

[5] K.J. Eskola, H. Paukkunen, C.A. Salgado, Nuclear PDFs at NLO - status report and review of the EPS09 results, Nucl. Phys. A 855 (2011).

[6] A. Majumder, M. Van Leeuwen, The theory and phenomenology of perturbative QCD based jet quenching, Prog. Part. Nucl. Phys. A 66 (2011).

[7] ALICE Collaboration, J. Adam, et al., Measurement of jet quenching with semi-inclusive hadron-jet distributions in central Pb–Pb collisions at $\sqrt{s_{NN}} = 2.76$ TeV, J. High Energy Phys. 09 (2015).

[8] STAR Collaboration, L. Adamczyk, et al., Measurements of jet quenching with semi-inclusive hadron+jet distributions in Au+Au collisions at $\sqrt{s_{NN}} = 200$ GeV, Phys. Rev. C 96 (2) (2017).

[9] CMS Collaboration, A.M. Sirunyan, et al., Study of jet quenching with $Z +$ jet correlations in Pb–Pb and pp collisions at $\sqrt{s_{NN}} = 5.02$ TeV, Phys. Rev. Lett. 119 (8) (2017).

[10] ATLAS Collaboration, M. Aaboud, et al., Measurement of photon–jet transverse momentum correlations in 5.02 TeV Pb + Pb and pp collisions with ATLAS, Phys. Lett. B 789 (2019).

[11] ALICE Collaboration, S. Acharya, et al., Medium modification of the shape of small-radius jets in central Pb–Pb collisions at $\sqrt{s_{NN}} = 2.76$ TeV, J. High Energy Phys. 10 (2018).

[12] CMS Collaboration, S. Chatrchyan, et al., Modification of jet shapes in Pb–Pb collisions at $\sqrt{s_{NN}} = 2.76$ TeV, Phys. Lett. B 730 (2014).

[13] CMS Collaboration, A.M. Sirunyan, et al., Observation of medium-induced modifications of jet fragmentation in Pb-Pb collisions at $\sqrt{s_{NN}} = 5.02$ TeV using isolated photon-tagged jets, Phys. Rev. Lett. 121 (24) (2018).

[14] ATLAS Collaboration, M. Aaboud, et al., Measurement of jet fragmentation in Pb+Pb and pp collisions at $\sqrt{s_{NN}} = 2.76$ TeV with the ATLAS detector at the LHC, Eur. Phys. J. C 77 (2017).

[15] ALICE Collaboration, S. Acharya, et al., First measurement of jet mass in Pb–Pb and p–Pb collisions at the LHC, Phys. Lett. B 776 (2018).

[16] CMS Collaboration, A.M. Sirunyan, et al., Measurement of the groomed jet mass in PbPb and pp collisions at $\sqrt{s_{NN}} = 5.02$ TeV, J. High Energy Phys. 10 (2018).

[17] K.M. Burke, A. Buzzatti, N. Chang, C. Gale, M. Gyulassy, et al., Extracting jet transport coefficient from jet quenching at RHIC and LHC, Phys. Rev. C 90 (2014).

[18] J.R. Andersen, et al., Les Houches 2017: Physics at TeV Colliders Standard Model Working Group Report.

[19] B. Andersson, G. Gustafson, L. Lonnblad, U. Pettersson, Coherence effects in deep inelastic scattering, Z. Phys. C 43 (1989).

[20] F.A. Dreyer, G.P. Salam, G. Soyez, The lund jet plane, J. High Energy Phys. 12 (2018).

[21] H. Andrews, et al., Novel tools and observables for jet physics in heavy-ion collisions.

[22] M. Dasgupta, A. Fregoso, S. Marzani, G.P. Salam, Towards an understanding of jet substructure, J. High Energy Phys. 09 (2013).

[23] A.J. Larkoski, S. Marzani, G. Soyez, J. Thaler, Soft drop, J. High Energy Phys. 05 (2014).

[24] G. Milhano, U.A. Wiedemann, K. Zapp, Sensitivity of jet substructure to jet-induced medium response, Phys. Lett. B 779 (2018).

[25] F. D'Eramo, K. Rajagopal, Y. Yin, Molière scattering in quark-gluon plasma: finding point-like scatterers in a liquid, J. High Energy Phys. 01 (2019).

[26] Y. Mehtar-Tani, K. Tywoniuk, Groomed jets in heavy-ion collisions: sensitivity to medium-induced bremsstrahlung, J. High Energy Phys. 04 (2017).

[27] N. Chang, S. Cao, G. Qin, Probing medium-induced jet splitting and energy loss in heavy-ion collisions, Phys. Lett. B 781 (2018).

[28] J. Casalderrey-Solana, Y. Mehtar-Tani, C.A. Salgado, K. Tywoniuk, New picture of jet quenching dictated by color coherence, Phys. Lett. B 725 (2013).

[29] CMS Collaboration, A.M. Sirunyan, et al., Measurement of the splitting function in pp and Pb–Pb collisions at $\sqrt{s_{NN}} = 5.02$ TeV, Phys. Rev. Lett. 120 (14) (2018).

[30] STAR Collaboration, K. Kauder, et al., Measurement of the shared momentum fraction z_g using jet reconstruction in p+p and Au+Au collisions with STAR, Nucl. Phys. A 967 (2017).

[31] C. Frye, A.J. Larkoski, J. Thaler, K. Zhou, Casimir meets Poisson: improved quark/gluon discrimination with counting observables, J. High Energy Phys. 09 (2017), arXiv:1704.06266 [hep-ph].

[32] ALICE Collaboration, K. Aamodt, et al., The ALICE experiment at the CERN LHC, J. Instrum. 3 (2008).

[33] ALICE Collaboration, B. Abelev, et al., Performance of the ALICE experiment at the CERN LHC, Int. J. Mod. Phys. A 29 (2014).

[34] ALICE Collaboration, B. Abelev, et al., Charged jet cross sections and properties in proton-proton collisions at $\sqrt{s} = 7$ TeV, Phys. Rev. D 91 (2015).

[35] ALICE Collaboration, E. Abbas, et al., Performance of the ALICE VZERO system, J. Instrum. 8 (2013).

[36] ALICE Collaboration, K. Aamodt, et al., Alignment of the ALICE inner tracking system with cosmic-ray tracks, J. Instrum. 5 (2010).

[37] K. Aamodt, et al., The ALICE TPC, a large 3-dimensional tracking device with fast readout for ultra-high multiplicity events, Nucl. Instrum. Methods Phys. Res. A 622 (Oct. 2010).

[38] ALICE Collaboration, J. Adam, et al., Measurement of jet suppression in central Pb–Pb collisions at $\sqrt{s_{NN}} = 2.76$ TeV, Phys. Lett. B 746 (2015).

[39] ALICE Collaboration, B. Abelev, et al., Centrality dependence of charged particle production at large transverse momentum in Pb–Pb collisions at $\sqrt{s_{NN}} = 2.76$ TeV, Phys. Lett. B 720 (2013).

[40] M. Cacciari, G.P. Salam, G. Soyez, The anti-k_t jet clustering algorithm, J. High Energy Phys. 04 (2008).

[41] M. Cacciari, G.P. Salam, G. Soyez, FastJet user manual, Eur. Phys. J. C 72 (2012).

[42] P. Berta, M. Spousta, D.W. Miller, R. Leitner, Particle-level pileup subtraction for jets and jet shapes, J. High Energy Phys. 06 (2014).

[43] S. Catani, Y. Dokshitzer, M. Seymour, B. Webber, Longitudinally-invariant k_t-clustering algorithms for hadron-hadron collisions, Nucl. Phys. B 406 (1) (1993).

[44] M. Cacciari, G.P. Salam, Dispelling the n3 myth for the k_t jet-finder, Phys. Lett. B 641 (1) (2006).

[45] Yu.L. Dokshitzer, G.D. Leder, S. Moretti, B.R. Webber, Better jet clustering algorithms, J. High Energy Phys. 08 (1997).

[46] R. Brun, F. Bruyant, M. Maire, A.C. McPherson, P. Zanarini, GEANT3 User's Guide, CERN Data Handling Division DD/EE/84-1, 1985.

[47] RooUnfold http://hepunx.rl.ac.uk/~adye/software/unfold/RooUnfold.html.

[48] J. Bellm, et al., Herwig 7.0/Herwig++ 3.0 release note, Eur. Phys. J. C 76 (4) (2016), arXiv:1512.01178 [hep-ph].

[49] S. Frixione, P. Nason, C. Oleari, Matching NLO QCD computations with parton shower simulations: the POWHEG method, J. High Energy Phys. 0711 (2007).

[50] T. Sjöstrand, S. Ask, J.R. Christiansen, R. Corke, N. Desai, P. Ilten, S. Mrenna, S. Prestel, C.O. Rasmussen, P.Z. Skands, An introduction to PYTHIA 8.2, Comput. Phys. Commun. 191 (2015).

[51] K. Zapp, G. Ingelman, J. Rathsman, J. Stachel, U.A. Wiedemann, A Monte Carlo model for 'jet quenching', Eur. Phys. J. C 60 (2009).

[52] J. Casalderrey-Solana, D.C. Gulhan, J.G. Milhano, D. Pablos, K. Rajagopal, Jet quenching within a hybrid strong/weak coupling approach, Nucl. Phys. A 931 (2014).

[53] R. Kunnawalkam Elayavalli, K.C. Zapp, Medium response in JEWEL and its impact on jet shape observables in heavy ion collisions, J. High Energy Phys. 07 (2017).

[54] R. Baier, Yu.L. Dokshitzer, S. Peigné, D. Schiff, Induced gluon radiation in a QCD medium, Phys. Lett. B 345 (1994).

[55] R. Baier, D. Schiff, B.G. Zakharov, Energy loss in perturbative QCD, Annu. Rev. Nucl. Part. Sci. 50 (2000).

ALICE Collaboration

S. Acharya [141], D. Adamová [93], S.P. Adhya [141], A. Adler [74], J. Adolfsson [80], M.M. Aggarwal [98], G. Aglieri Rinella [34], M. Agnello [31], N. Agrawal [48,10], Z. Ahammed [141], S. Ahmad [17], S.U. Ahn [76], A. Akindinov [64], M. Al-Turany [105], S.N. Alam [141], D.S.D. Albuquerque [122], D. Aleksandrov [87], B. Alessandro [58], H.M. Alfanda [6], R. Alfaro Molina [72], B. Ali [17], Y. Ali [15], A. Alici [10,53,27], A. Alkin [2], J. Alme [22], T. Alt [69], L. Altenkamper [22], I. Altsybeev [112], M.N. Anaam [6], C. Andrei [47], D. Andreou [34], H.A. Andrews [109], A. Andronic [144], M. Angeletti [34], V. Anguelov [102], C. Anson [16], T. Antičić [106], F. Antinori [56], P. Antonioli [53], R. Anwar [126], N. Apadula [79], L. Aphecetche [114], H. Appelshäuser [69], S. Arcelli [27], R. Arnaldi [58], M. Arratia [79], I.C. Arsene [21], M. Arslandok [102], A. Augustinus [34], R. Averbeck [105], S. Aziz [61], M.D. Azmi [17], A. Badalà [55], Y.W. Baek [40], S. Bagnasco [58], X. Bai [105], R. Bailhache [69], R. Bala [99], A. Baldisseri [137], M. Ball [42], S. Balouza [103], R.C. Baral [85], R. Barbera [28], L. Barioglio [26], G.G. Barnaföldi [145], L.S. Barnby [92], V. Barret [134], P. Bartalini [6], K. Barth [34], E. Bartsch [69], F. Baruffaldi [29], N. Bastid [134], S. Basu [143], G. Batigne [114], B. Batyunya [75], P.C. Batzing [21], D. Bauri [48], J.L. Bazo Alba [110], I.G. Bearden [88], C. Bedda [63], N.K. Behera [60], I. Belikov [136], F. Bellini [34], R. Bellwied [126], V. Belyaev [91], G. Bencedi [145], S. Beole [26], A. Bercuci [47], Y. Berdnikov [96], D. Berenyi [145], R.A. Bertens [130], D. Berzano [58], M.G. Besoiu [68], L. Betev [34], A. Bhasin [99], I.R. Bhat [99], H. Bhatt [48], B. Bhattacharjee [41], A. Bianchi [26], L. Bianchi [126,26], N. Bianchi [51], J. Bielčík [37], J. Bielčíková [93], A. Bilandzic [117,103], G. Biro [145], R. Biswas [3], S. Biswas [3],

J.T. Blair [119], D. Blau [87], C. Blume [69], G. Boca [139], F. Bock [94,34], A. Bogdanov [91], L. Boldizsár [145],
A. Bolozdynya [91], M. Bombara [38], G. Bonomi [140], H. Borel [137], A. Borissov [144,91], M. Borri [128], H. Bossi [146],
E. Botta [26], C. Bourjau [88], L. Bratrud [69], P. Braun-Munzinger [105], M. Bregant [121], T.A. Broker [69], M. Broz [37],
E.J. Brucken [43], E. Bruna [58], G.E. Bruno [33,104], M.D. Buckland [128], D. Budnikov [107], H. Buesching [69],
S. Bufalino [31], O. Bugnon [114], P. Buhler [113], P. Buncic [34], Z. Buthelezi [73], J.B. Butt [15], J.T. Buxton [95],
D. Caffarri [89], A. Caliva [105], E. Calvo Villar [110], R.S. Camacho [44], P. Camerini [25], A.A. Capon [113],
F. Carnesecchi [10], J. Castillo Castellanos [137], A.J. Castro [130], E.A.R. Casula [54], F. Catalano [31],
C. Ceballos Sanchez [52], P. Chakraborty [48], S. Chandra [141], B. Chang [127], W. Chang [6], S. Chapeland [34],
M. Chartier [128], S. Chattopadhyay [141], S. Chattopadhyay [108], A. Chauvin [24], C. Cheshkov [135], B. Cheynis [135],
V. Chibante Barroso [34], D.D. Chinellato [122], S. Cho [60], P. Chochula [34], T. Chowdhury [134], P. Christakoglou [89],
C.H. Christensen [88], P. Christiansen [80], T. Chujo [133], C. Cicalo [54], L. Cifarelli [10,27], F. Cindolo [53],
J. Cleymans [125], F. Colamaria [52], D. Colella [52], A. Collu [79], M. Colocci [27], M. Concas [58,ii],
G. Conesa Balbastre [78], Z. Conesa del Valle [61], G. Contin [59,128], J.G. Contreras [37], T.M. Cormier [94],
Y. Corrales Morales [58,26], P. Cortese [32], M.R. Cosentino [123], F. Costa [34], S. Costanza [139], J. Crkovská [61],
P. Crochet [134], E. Cuautle [70], L. Cunqueiro [94], D. Dabrowski [142], T. Dahms [103,117], A. Dainese [56],
F.P.A. Damas [137,114], S. Dani [66], M.C. Danisch [102], A. Danu [68], D. Das [108], I. Das [108], S. Das [3], A. Dash [85],
S. Dash [48], A. Dashi [103], S. De [85,49], A. De Caro [30], G. de Cataldo [52], C. de Conti [121], J. de Cuveland [39],
A. De Falco [24], D. De Gruttola [10], N. De Marco [58], S. De Pasquale [30], R.D. De Souza [122], S. Deb [49],
H.F. Degenhardt [121], K.R. Deja [142], A. Deloff [84], S. Delsanto [131,26], P. Dhankher [48], D. Di Bari [33],
A. Di Mauro [34], R.A. Diaz [8], T. Dietel [125], P. Dillenseger [69], Y. Ding [6], R. Divià [34], Ø. Djuvsland [22],
U. Dmitrieva [62], A. Dobrin [34,68], B. Dönigus [69], O. Dordic [21], A.K. Dubey [141], A. Dubla [105], S. Dudi [98],
M. Dukhishyam [85], P. Dupieux [134], R.J. Ehlers [146], D. Elia [52], H. Engel [74], E. Epple [146], B. Erazmus [114],
F. Erhardt [97], A. Erokhin [112], M.R. Ersdal [22], B. Espagnon [61], G. Eulisse [34], J. Eum [18], D. Evans [109],
S. Evdokimov [90], L. Fabbietti [117,103], M. Faggin [29], J. Faivre [78], A. Fantoni [51], M. Fasel [94], P. Fecchio [31],
L. Feldkamp [144], A. Feliciello [58], G. Feofilov [112], A. Fernández Téllez [44], A. Ferrero [137], A. Ferretti [26],
A. Festanti [34], V.J.G. Feuillard [102], J. Figiel [118], S. Filchagin [107], D. Finogeev [62], F.M. Fionda [22], G. Fiorenza [52],
F. Flor [126], S. Foertsch [73], P. Foka [105], S. Fokin [87], E. Fragiacomo [59], U. Frankenfeld [105], G.G. Fronze [26],
U. Fuchs [34], C. Furget [78], A. Furs [62], M. Fusco Girard [30], J.J. Gaardhøje [88], M. Gagliardi [26], A.M. Gago [110],
A. Gal [136], C.D. Galvan [120], P. Ganoti [83], C. Garabatos [105], E. Garcia-Solis [11], K. Garg [28], C. Gargiulo [34],
A. Garibli [86], K. Garner [144], P. Gasik [103,117], E.F. Gauger [119], M.B. Gay Ducati [71], M. Germain [114],
J. Ghosh [108], P. Ghosh [141], S.K. Ghosh [3], P. Gianotti [51], P. Giubellino [105,58], P. Giubilato [29], P. Glässel [102],
D.M. Gómez Coral [72], A. Gomez Ramirez [74], V. Gonzalez [105], P. González-Zamora [44], S. Gorbunov [39],
L. Görlich [118], S. Gotovac [35], V. Grabski [72], L.K. Graczykowski [142], K.L. Graham [109], L. Greiner [79], A. Grelli [63],
C. Grigoras [34], V. Grigoriev [91], A. Grigoryan [1], S. Grigoryan [75], O.S. Groettvik [22], J.M. Gronefeld [105],
F. Grosa [31], J.F. Grosse-Oetringhaus [34], R. Grosso [105], R. Guernane [78], B. Guerzoni [27], M. Guittiere [114],
K. Gulbrandsen [88], T. Gunji [132], A. Gupta [99], R. Gupta [99], I.B. Guzman [44], R. Haake [34,146], M.K. Habib [105],
C. Hadjidakis [61], H. Hamagaki [81], G. Hamar [145], M. Hamid [6], R. Hannigan [119], M.R. Haque [63],
A. Harlenderova [105], J.W. Harris [146], A. Harton [11], J.A. Hasenbichler [34], H. Hassan [78], D. Hatzifotiadou [10,53],
P. Hauer [42], S. Hayashi [132], S.T. Heckel [69], E. Hellbär [69], H. Helstrup [36], A. Herghelegiu [47],
E.G. Hernandez [44], G. Herrera Corral [9], F. Herrmann [144], K.F. Hetland [36], T.E. Hilden [43], H. Hillemanns [34],
C. Hills [128], B. Hippolyte [136], B. Hohlweger [103], D. Horak [37], S. Hornung [105], R. Hosokawa [133], P. Hristov [34],
C. Huang [61], C. Hughes [130], P. Huhn [69], T.J. Humanic [95], H. Hushnud [108], L.A. Husova [144], N. Hussain [41],
S.A. Hussain [15], T. Hussain [17], D. Hutter [39], D.S. Hwang [19], J.P. Iddon [128,34], R. Ilkaev [107], M. Inaba [133],
M. Ippolitov [87], M.S. Islam [108], M. Ivanov [105], V. Ivanov [96], V. Izucheev [90], B. Jacak [79], N. Jacazio [27],
P.M. Jacobs [79], M.B. Jadhav [48], S. Jadlovska [116], J. Jadlovsky [116], S. Jaelani [63], C. Jahnke [121],
M.J. Jakubowska [142], M.A. Janik [142], M. Jercic [97], O. Jevons [109], R.T. Jimenez Bustamante [105], M. Jin [126],
F. Jonas [144,94], P.G. Jones [109], A. Jusko [109], P. Kalinak [65], A. Kalweit [34], J.H. Kang [147], V. Kaplin [91], S. Kar [6],
A. Karasu Uysal [77], O. Karavichev [62], T. Karavicheva [62], P. Karczmarczyk [34], E. Karpechev [62],
U. Kebschull [74], R. Keidel [46], M. Keil [34], B. Ketzer [42], Z. Khabanova [89], A.M. Khan [6], S. Khan [17],
S.A. Khan [141], A. Khanzadeev [96], Y. Kharlov [90], A. Khatun [17], A. Khuntia [118,49], B. Kileng [36], B. Kim [60],
B. Kim [133], D. Kim [147], D.J. Kim [127], E.J. Kim [13], H. Kim [147], J. Kim [147], J.S. Kim [40], J. Kim [102], J. Kim [147],
J. Kim [13], M. Kim [102], S. Kim [19], T. Kim [147], T. Kim [147], S. Kirsch [39], I. Kisel [39], S. Kiselev [64], A. Kisiel [142],

J.L. Klay [5], C. Klein [69], J. Klein [58], S. Klein [79], C. Klein-Bösing [144], S. Klewin [102], A. Kluge [34], M.L. Knichel [34], A.G. Knospe [126], C. Kobdaj [115], M.K. Köhler [102], T. Kollegger [105], A. Kondratyev [75], N. Kondratyeva [91], E. Kondratyuk [90], P.J. Konopka [34], L. Koska [116], O. Kovalenko [84], V. Kovalenko [112], M. Kowalski [118], I. Králik [65], A. Kravčáková [38], L. Kreis [105], M. Krivda [65,109], F. Krizek [93], K. Krizkova Gajdosova [37], M. Krüger [69], E. Kryshen [96], M. Krzewicki [39], A.M. Kubera [95], V. Kučera [60], C. Kuhn [136], P.G. Kuijer [89], L. Kumar [98], S. Kumar [48], S. Kundu [85], P. Kurashvili [84], A. Kurepin [62], A.B. Kurepin [62], S. Kushpil [93], J. Kvapil [109], M.J. Kweon [60], J.Y. Kwon [60], Y. Kwon [147], S.L. La Pointe [39], P. La Rocca [28], Y.S. Lai [79], R. Langoy [124], K. Lapidus [34,146], A. Lardeux [21], P. Larionov [51], E. Laudi [34], R. Lavicka [37], T. Lazareva [112], R. Lea [25], L. Leardini [102], S. Lee [147], F. Lehas [89], S. Lehner [113], J. Lehrbach [39], R.C. Lemmon [92], I. León Monzón [120], E.D. Lesser [20], M. Lettrich [34], P. Lévai [145], X. Li [12], X.L. Li [6], J. Lien [124], R. Lietava [109], B. Lim [18], S. Lindal [21], V. Lindenstruth [39], S.W. Lindsay [128], C. Lippmann [105], M.A. Lisa [95], V. Litichevskyi [43], A. Liu [79], S. Liu [95], W.J. Llope [143], I.M. Lofnes [22], V. Loginov [91], C. Loizides [94], P. Loncar [35], X. Lopez [134], E. López Torres [8], P. Luettig [69], J.R. Luhder [144], M. Lunardon [29], G. Luparello [59], M. Lupi [74], A. Maevskaya [62], M. Mager [34], S.M. Mahmood [21], T. Mahmoud [42], A. Maire [136], R.D. Majka [146], M. Malaev [96], Q.W. Malik [21], L. Malinina [75,iii], D. Mal'Kevich [64], P. Malzacher [105], A. Mamonov [107], V. Manko [87], F. Manso [134], V. Manzari [52], Y. Mao [6], M. Marchisone [135], J. Mareš [67], G.V. Margagliotti [25], A. Margotti [53], J. Margutti [63], A. Marín [105], C. Markert [119], M. Marquard [69], N.A. Martin [102], P. Martinengo [34], J.L. Martinez [126], M.I. Martínez [44], G. Martínez García [114], M. Martinez Pedreira [34], S. Masciocchi [105], M. Masera [26], A. Masoni [54], L. Massacrier [61], E. Masson [114], A. Mastroserio [138,52], A.M. Mathis [103,117], P.F.T. Matuoka [121], A. Matyja [118], C. Mayer [118], M. Mazzilli [33], M.A. Mazzoni [57], A.F. Mechler [69], F. Meddi [23], Y. Melikyan [91], A. Menchaca-Rocha [72], E. Meninno [30], M. Meres [14], S. Mhlanga [125], Y. Miake [133], L. Micheletti [26], M.M. Mieskolainen [43], D.L. Mihaylov [103], K. Mikhaylov [64,75], A. Mischke [63,i], A.N. Mishra [70], D. Miśkowiec [105], C.M. Mitu [68], N. Mohammadi [34], A.P. Mohanty [63], B. Mohanty [85], M. Mohisin Khan [17,iv], M. Mondal [141], M.M. Mondal [66], C. Mordasini [103], D.A. Moreira De Godoy [144], L.A.P. Moreno [44], S. Moretto [29], A. Morreale [114], A. Morsch [34], T. Mrnjavac [34], V. Muccifora [51], E. Mudnic [35], D. Mühlheim [144], S. Muhuri [141], J.D. Mulligan [146,79], M.G. Munhoz [121], K. Münning [42], R.H. Munzer [69], H. Murakami [132], S. Murray [73], L. Musa [34], J. Musinsky [65], C.J. Myers [126], J.W. Myrcha [142], B. Naik [48], R. Nair [84], B.K. Nandi [48], R. Nania [53,10], E. Nappi [52], M.U. Naru [15], A.F. Nassirpour [80], H. Natal da Luz [121], C. Nattrass [130], R. Nayak [48], T.K. Nayak [141,85], S. Nazarenko [107], R.A. Negrao De Oliveira [69], L. Nellen [70], S.V. Nesbo [36], G. Neskovic [39], B.S. Nielsen [88], S. Nikolaev [87], S. Nikulin [87], V. Nikulin [96], F. Noferini [10,53], P. Nomokonov [75], G. Nooren [63], J. Norman [78], P. Nowakowski [142], A. Nyanin [87], J. Nystrand [22], M. Ogino [81], A. Ohlson [102], J. Oleniacz [142], A.C. Oliveira Da Silva [121], M.H. Oliver [146], C. Oppedisano [58], R. Orava [43], A. Ortiz Velasquez [70], A. Oskarsson [80], J. Otwinowski [118], K. Oyama [81], Y. Pachmayer [102], V. Pacik [88], D. Pagano [140], G. Paić [70], P. Palni [6], J. Pan [143], A.K. Pandey [48], S. Panebianco [137], V. Papikyan [1], P. Pareek [49], J. Park [60], J.E. Parkkila [127], S. Parmar [98], A. Passfeld [144], S.P. Pathak [126], R.N. Patra [141], B. Paul [24,58], H. Pei [6], T. Peitzmann [63], X. Peng [6], L.G. Pereira [71], H. Pereira Da Costa [137], D. Peresunko [87], G.M. Perez [8], E. Perez Lezama [69], V. Peskov [69], Y. Pestov [4], V. Petráček [37], M. Petrovici [47], R.P. Pezzi [71], S. Piano [59], M. Pikna [14], P. Pillot [114], L.O.D.L. Pimentel [88], O. Pinazza [53,34], L. Pinsky [126], S. Pisano [51], D.B. Piyarathna [126], M. Płoskoń [79], M. Planinic [97], F. Pliquett [69], J. Pluta [142], S. Pochybova [145], M.G. Poghosyan [94], B. Polichtchouk [90], N. Poljak [97], W. Poonsawat [115], A. Pop [47], H. Poppenborg [144], S. Porteboeuf-Houssais [134], V. Pozdniakov [75], S.K. Prasad [3], R. Preghenella [53], F. Prino [58], C.A. Pruneau [143], I. Pshenichnov [62], M. Puccio [34,26], V. Punin [107], K. Puranapanda [141], J. Putschke [143], R.E. Quishpe [126], S. Ragoni [109], S. Raha [3], S. Rajput [99], J. Rak [127], A. Rakotozafindrabe [137], L. Ramello [32], F. Rami [136], R. Raniwala [100], S. Raniwala [100], S.S. Räsänen [43], B.T. Rascanu [69], R. Rath [49], V. Ratza [42], I. Ravasenga [31], K.F. Read [130,94], K. Redlich [84,v], A. Rehman [22], P. Reichelt [69], F. Reidt [34], X. Ren [6], R. Renfordt [69], A. Reshetin [62], J.-P. Revol [10], K. Reygers [102], V. Riabov [96], T. Richert [80,88], M. Richter [21], P. Riedler [34], W. Riegler [34], F. Riggi [28], C. Ristea [68], S.P. Rode [49], M. Rodríguez Cahuantzi [44], K. Røed [21], R. Rogalev [90], E. Rogochaya [75], D. Rohr [34], D. Röhrich [22], P.S. Rokita [142], F. Ronchetti [51], E.D. Rosas [70], K. Roslon [142], P. Rosnet [134], A. Rossi [29], A. Rotondi [139], F. Roukoutakis [83], A. Roy [49], P. Roy [108], O.V. Rueda [80], R. Rui [25], B. Rumyantsev [75], A. Rustamov [86], E. Ryabinkin [87], Y. Ryabov [96], A. Rybicki [118], H. Rytkonen [127], S. Saarinen [43], S. Sadhu [141], S. Sadovsky [90], K. Šafařík [37,34], S.K. Saha [141], B. Sahoo [48], P. Sahoo [49], R. Sahoo [49], S. Sahoo [66], P.K. Sahu [66], J. Saini [141], S. Sakai [133], S. Sambyal [99], V. Samsonov [96,91],

A. Sandoval [72], A. Sarkar [73], D. Sarkar [141,143], N. Sarkar [141], P. Sarma [41], V.M. Sarti [103], M.H.P. Sas [63], E. Scapparone [53], B. Schaefer [94], J. Schambach [119], H.S. Scheid [69], C. Schiaua [47], R. Schicker [102], A. Schmah [102], C. Schmidt [105], H.R. Schmidt [101], M.O. Schmidt [102], M. Schmidt [101], N.V. Schmidt [94,69], A.R. Schmier [130], J. Schukraft [34,88], Y. Schutz [34,136], K. Schwarz [105], K. Schweda [105], G. Scioli [27], E. Scomparin [58], M. Šefčík [38], J.E. Seger [16], Y. Sekiguchi [132], D. Sekihata [132,45], I. Selyuzhenkov [105,91], S. Senyukov [136], D. Serebryakov [62], E. Serradilla [72], P. Sett [48], A. Sevcenco [68], A. Shabanov [62], A. Shabetai [114], R. Shahoyan [34], W. Shaikh [108], A. Shangaraev [90], A. Sharma [98], A. Sharma [99], M. Sharma [99], N. Sharma [98], A.I. Sheikh [141], K. Shigaki [45], M. Shimomura [82], S. Shirinkin [64], Q. Shou [111], Y. Sibiriak [87], S. Siddhanta [54], T. Siemiarczuk [84], D. Silvermyr [80], C. Silvestre [78], G. Simatovic [89], G. Simonetti [34,103], R. Singh [85], R. Singh [99], V.K. Singh [141], V. Singhal [141], T. Sinha [108], B. Sitar [14], M. Sitta [32], T.B. Skaali [21], M. Slupecki [127], N. Smirnov [146], R.J.M. Snellings [63], T.W. Snellman [127], J. Sochan [116], C. Soncco [110], J. Song [60,126], A. Songmoolnak [115], F. Soramel [29], S. Sorensen [130], I. Sputowska [118], J. Stachel [102], I. Stan [68], P. Stankus [94], P.J. Steffanic [130], E. Stenlund [80], D. Stocco [114], M.M. Storetvedt [36], P. Strmen [14], A.A.P. Suaide [121], T. Sugitate [45], C. Suire [61], M. Suleymanov [15], M. Suljic [34], R. Sultanov [64], M. Šumbera [93], S. Sumowidagdo [50], K. Suzuki [113], S. Swain [66], A. Szabo [14], I. Szarka [14], U. Tabassam [15], G. Taillepied [134], J. Takahashi [122], G.J. Tambave [22], S. Tang [134,6], M. Tarhini [114], M.G. Tarzila [47], A. Tauro [34], G. Tejeda Muñoz [44], A. Telesca [34], C. Terrevoli [126,29], D. Thakur [49], S. Thakur [141], D. Thomas [119], F. Thoresen [88], R. Tieulent [135], A. Tikhonov [62], A.R. Timmins [126], A. Toia [69], N. Topilskaya [62], M. Toppi [51], F. Torales-Acosta [20], S.R. Torres [120], S. Tripathy [49], T. Tripathy [48], S. Trogolo [26,29], G. Trombetta [33], L. Tropp [38], V. Trubnikov [2], W.H. Trzaska [127], T.P. Trzcinski [142], B.A. Trzeciak [63], T. Tsuji [132], A. Tumkin [107], R. Turrisi [56], T.S. Tveter [21], K. Ullaland [22], E.N. Umaka [126], A. Uras [135], G.L. Usai [24], A. Utrobicic [97], M. Vala [116,38], N. Valle [139], S. Vallero [58], N. van der Kolk [63], L.V.R. van Doremalen [63], M. van Leeuwen [63], P. Vande Vyvre [34], D. Varga [145], M. Varga-Kofarago [145], A. Vargas [44], M. Vargyas [127], R. Varma [48], M. Vasileiou [83], A. Vasiliev [87], O. Vázquez Doce [117,103], V. Vechernin [112], A.M. Veen [63], E. Vercellin [26], S. Vergara Limón [44], L. Vermunt [63], R. Vernet [7], R. Vértesi [145], M.G.D.L.C. Vicencio [9], L. Vickovic [35], J. Viinikainen [127], Z. Vilakazi [131], O. Villalobos Baillie [109], A. Villatoro Tello [44], G. Vino [52], A. Vinogradov [87], T. Virgili [30], V. Vislavicius [88], A. Vodopyanov [75], B. Volkel [34], M.A. Völkl [101], K. Voloshin [64], S.A. Voloshin [143], G. Volpe [33], B. von Haller [34], I. Vorobyev [103], D. Voscek [116], J. Vrláková [38], B. Wagner [22], Y. Watanabe [133], M. Weber [113], S.G. Weber [144,105], A. Wegrzynek [34], D.F. Weiser [102], S.C. Wenzel [34], J.P. Wessels [144], E. Widmann [113], J. Wiechula [69], J. Wikne [21], G. Wilk [84], J. Wilkinson [53], G.A. Willems [34], E. Willsher [109], B. Windelband [102], W.E. Witt [130], Y. Wu [129], R. Xu [6], S. Yalcin [77], K. Yamakawa [45], S. Yang [22], S. Yano [137], Z. Yin [6], H. Yokoyama [63], I.-K. Yoo [18], J.H. Yoon [60], S. Yuan [22], A. Yuncu [102], V. Yurchenko [2], V. Zaccolo [58,25], A. Zaman [15], C. Zampolli [34], H.J.C. Zanoli [121], N. Zardoshti [34], A. Zarochentsev [112], P. Závada [67], N. Zaviyalov [107], H. Zbroszczyk [142], M. Zhalov [96], X. Zhang [6], Z. Zhang [6,134], C. Zhao [21], V. Zherebchevskii [112], N. Zhigareva [64], D. Zhou [6], Y. Zhou [88], Z. Zhou [22], J. Zhu [6], Y. Zhu [6], A. Zichichi [27,10], M.B. Zimmermann [34], G. Zinovjev [2], N. Zurlo [140]

1 *A.I. Alikhanyan National Science Laboratory (Yerevan Physics Institute) Foundation, Yerevan, Armenia*
2 *Bogolyubov Institute for Theoretical Physics, National Academy of Sciences of Ukraine, Kiev, Ukraine*
3 *Bose Institute, Department of Physics and Centre for Astroparticle Physics and Space Science (CAPSS), Kolkata, India*
4 *Budker Institute for Nuclear Physics, Novosibirsk, Russia*
5 *California Polytechnic State University, San Luis Obispo, CA, United States*
6 *Central China Normal University, Wuhan, China*
7 *Centre de Calcul de l'IN2P3, Villeurbanne, Lyon, France*
8 *Centro de Aplicaciones Tecnológicas y Desarrollo Nuclear (CEADEN), Havana, Cuba*
9 *Centro de Investigación y de Estudios Avanzados (CINVESTAV), Mexico City and Mérida, Mexico*
10 *Centro Fermi – Museo Storico della Fisica e Centro Studi e Ricerche "Enrico Fermi", Rome, Italy*
11 *Chicago State University, Chicago, IL, United States*
12 *China Institute of Atomic Energy, Beijing, China*
13 *Chonbuk National University, Jeonju, Republic of Korea*
14 *Comenius University Bratislava, Faculty of Mathematics, Physics and Informatics, Bratislava, Slovakia*
15 *COMSATS University Islamabad, Islamabad, Pakistan*
16 *Creighton University, Omaha, NE, United States*
17 *Department of Physics, Aligarh Muslim University, Aligarh, India*
18 *Department of Physics, Pusan National University, Pusan, Republic of Korea*
19 *Department of Physics, Sejong University, Seoul, Republic of Korea*
20 *Department of Physics, University of California, Berkeley, CA, United States*
21 *Department of Physics, University of Oslo, Oslo, Norway*
22 *Department of Physics and Technology, University of Bergen, Bergen, Norway*
23 *Dipartimento di Fisica dell'Università 'La Sapienza' and Sezione INFN, Rome, Italy*
24 *Dipartimento di Fisica dell'Università and Sezione INFN, Cagliari, Italy*

[25] *Dipartimento di Fisica dell'Università and Sezione INFN, Trieste, Italy*
[26] *Dipartimento di Fisica dell'Università and Sezione INFN, Turin, Italy*
[27] *Dipartimento di Fisica e Astronomia dell'Università and Sezione INFN, Bologna, Italy*
[28] *Dipartimento di Fisica e Astronomia dell'Università and Sezione INFN, Catania, Italy*
[29] *Dipartimento di Fisica e Astronomia dell'Università and Sezione INFN, Padova, Italy*
[30] *Dipartimento di Fisica 'E.R. Caianiello' dell'Università and Gruppo Collegato INFN, Salerno, Italy*
[31] *Dipartimento DISAT del Politecnico and Sezione INFN, Turin, Italy*
[32] *Dipartimento di Scienze e Innovazione Tecnologica dell'Università del Piemonte Orientale and INFN Sezione di Torino, Alessandria, Italy*
[33] *Dipartimento Interateneo di Fisica 'M. Merlin' and Sezione INFN, Bari, Italy*
[34] *European Organization for Nuclear Research (CERN), Geneva, Switzerland*
[35] *Faculty of Electrical Engineering, Mechanical Engineering and Naval Architecture, University of Split, Split, Croatia*
[36] *Faculty of Engineering and Science, Western Norway University of Applied Sciences, Bergen, Norway*
[37] *Faculty of Nuclear Sciences and Physical Engineering, Czech Technical University in Prague, Prague, Czech Republic*
[38] *Faculty of Science, P.J. Šafárik University, Košice, Slovakia*
[39] *Frankfurt Institute for Advanced Studies, Johann Wolfgang Goethe-Universität Frankfurt, Frankfurt, Germany*
[40] *Gangneung-Wonju National University, Gangneung, Republic of Korea*
[41] *Gauhati University, Department of Physics, Guwahati, India*
[42] *Helmholtz-Institut für Strahlen- und Kernphysik, Rheinische Friedrich-Wilhelms-Universität Bonn, Bonn, Germany*
[43] *Helsinki Institute of Physics (HIP), Helsinki, Finland*
[44] *High Energy Physics Group, Universidad Autónoma de Puebla, Puebla, Mexico*
[45] *Hiroshima University, Hiroshima, Japan*
[46] *Hochschule Worms, Zentrum für Technologietransfer und Telekommunikation (ZTT), Worms, Germany*
[47] *Horia Hulubei National Institute of Physics and Nuclear Engineering, Bucharest, Romania*
[48] *Indian Institute of Technology Bombay (IIT), Mumbai, India*
[49] *Indian Institute of Technology Indore, Indore, India*
[50] *Indonesian Institute of Sciences, Jakarta, Indonesia*
[51] *INFN, Laboratori Nazionali di Frascati, Frascati, Italy*
[52] *INFN, Sezione di Bari, Bari, Italy*
[53] *INFN, Sezione di Bologna, Bologna, Italy*
[54] *INFN, Sezione di Cagliari, Cagliari, Italy*
[55] *INFN, Sezione di Catania, Catania, Italy*
[56] *INFN, Sezione di Padova, Padova, Italy*
[57] *INFN, Sezione di Roma, Rome, Italy*
[58] *INFN, Sezione di Torino, Turin, Italy*
[59] *INFN, Sezione di Trieste, Trieste, Italy*
[60] *Inha University, Incheon, Republic of Korea*
[61] *Institut de Physique Nucléaire d'Orsay (IPNO), Institut National de Physique Nucléaire et de Physique des Particules (IN2P3/CNRS), Université de Paris-Sud, Université Paris-Saclay, Orsay, France*
[62] *Institute for Nuclear Research, Academy of Sciences, Moscow, Russia*
[63] *Institute for Subatomic Physics, Utrecht University/Nikhef, Utrecht, Netherlands*
[64] *Institute for Theoretical and Experimental Physics, Moscow, Russia*
[65] *Institute of Experimental Physics, Slovak Academy of Sciences, Košice, Slovakia*
[66] *Institute of Physics, Homi Bhabha National Institute, Bhubaneswar, India*
[67] *Institute of Physics of the Czech Academy of Sciences, Prague, Czech Republic*
[68] *Institute of Space Science (ISS), Bucharest, Romania*
[69] *Institut für Kernphysik, Johann Wolfgang Goethe, Universität Frankfurt, Frankfurt, Germany*
[70] *Instituto de Ciencias Nucleares, Universidad Nacional Autónoma de México, Mexico City, Mexico*
[71] *Instituto de Física, Universidade Federal do Rio Grande do Sul (UFRGS), Porto Alegre, Brazil*
[72] *Instituto de Física, Universidad Nacional Autónoma de México, Mexico City, Mexico*
[73] *iThemba LABS, National Research Foundation, Somerset West, South Africa*
[74] *Johann-Wolfgang-Goethe Universität Frankfurt, Institut für Informatik, Fachbereich Informatik und Mathematik, Frankfurt, Germany*
[75] *Joint Institute for Nuclear Research (JINR), Dubna, Russia*
[76] *Korea Institute of Science and Technology Information, Daejeon, Republic of Korea*
[77] *KTO Karatay University, Konya, Turkey*
[78] *Laboratoire de Physique Subatomique et de Cosmologie, Université Grenoble-Alpes, CNRS-IN2P3, Grenoble, France*
[79] *Lawrence Berkeley National Laboratory, Berkeley, CA, United States*
[80] *Lund University Department of Physics, Division of Particle Physics, Lund, Sweden*
[81] *Nagasaki Institute of Applied Science, Nagasaki, Japan*
[82] *Nara Women's University (NWU), Nara, Japan*
[83] *National and Kapodistrian University of Athens, School of Science, Department of Physics, Athens, Greece*
[84] *National Centre for Nuclear Research, Warsaw, Poland*
[85] *National Institute of Science Education and Research, Homi Bhabha National Institute, Jatni, India*
[86] *National Nuclear Research Center, Baku, Azerbaijan*
[87] *National Research Centre Kurchatov Institute, Moscow, Russia*
[88] *Niels Bohr Institute, University of Copenhagen, Copenhagen, Denmark*
[89] *NIKHEF, National Institute for Subatomic Physics, Amsterdam, Netherlands*
[90] *NRC Kurchatov Institute IHEP, Protvino, Russia*
[91] *NRNU Moscow Engineering Physics Institute, Moscow, Russia*
[92] *Nuclear Physics Group, STFC Daresbury Laboratory, Daresbury, United Kingdom*
[93] *Nuclear Physics Institute of the Czech Academy of Sciences, Řež u Prahy, Czech Republic*
[94] *Oak Ridge National Laboratory, Oak Ridge, TN, United States*
[95] *Ohio State University, Columbus, OH, United States*
[96] *Petersburg Nuclear Physics Institute, Gatchina, Russia*
[97] *Physics Department, Faculty of Science, University of Zagreb, Zagreb, Croatia*
[98] *Physics Department, Panjab University, Chandigarh, India*
[99] *Physics Department, University of Jammu, Jammu, India*
[100] *Physics Department, University of Rajasthan, Jaipur, India*
[101] *Physikalisches Institut, Eberhard-Karls-Universität Tübingen, Tübingen, Germany*
[102] *Physikalisches Institut, Ruprecht-Karls-Universität Heidelberg, Heidelberg, Germany*

[103] *Physik Department, Technische Universität München, Munich, Germany*
[104] *Politecnico di Bari, Bari, Italy*
[105] *Research Division and ExtreMe Matter Institute EMMI, GSI Helmholtzzentrum für Schwerionenforschung GmbH, Darmstadt, Germany*
[106] *Rudjer Bošković Institute, Zagreb, Croatia*
[107] *Russian Federal Nuclear Center (VNIIEF), Sarov, Russia*
[108] *Saha Institute of Nuclear Physics, Homi Bhabha National Institute, Kolkata, India*
[109] *School of Physics and Astronomy, University of Birmingham, Birmingham, United Kingdom*
[110] *Sección Física, Departamento de Ciencias, Pontificia Universidad Católica del Perú, Lima, Peru*
[111] *Shanghai Institute of Applied Physics, Shanghai, China*
[112] *St. Petersburg State University, St. Petersburg, Russia*
[113] *Stefan Meyer Institut für Subatomare Physik (SMI), Vienna, Austria*
[114] *SUBATECH, IMT Atlantique, Université de Nantes, CNRS-IN2P3, Nantes, France*
[115] *Suranaree University of Technology, Nakhon Ratchasima, Thailand*
[116] *Technical University of Košice, Košice, Slovakia*
[117] *Technische Universität München, Excellence Cluster 'Universe', Munich, Germany*
[118] *The Henryk Niewodniczanski Institute of Nuclear Physics, Polish Academy of Sciences, Cracow, Poland*
[119] *The University of Texas at Austin, Austin, TX, United States*
[120] *Universidad Autónoma de Sinaloa, Culiacán, Mexico*
[121] *Universidade de São Paulo (USP), São Paulo, Brazil*
[122] *Universidade Estadual de Campinas (UNICAMP), Campinas, Brazil*
[123] *Universidade Federal do ABC, Santo Andre, Brazil*
[124] *University College of Southeast Norway, Tonsberg, Norway*
[125] *University of Cape Town, Cape Town, South Africa*
[126] *University of Houston, Houston, TX, United States*
[127] *University of Jyväskylä, Jyväskylä, Finland*
[128] *University of Liverpool, Liverpool, United Kingdom*
[129] *University of Science and Techonology of China, Hefei, China*
[130] *University of Tennessee, Knoxville, TN, United States*
[131] *University of the Witwatersrand, Johannesburg, South Africa*
[132] *University of Tokyo, Tokyo, Japan*
[133] *University of Tsukuba, Tsukuba, Japan*
[134] *Université Clermont Auvergne, CNRS/IN2P3, LPC, Clermont-Ferrand, France*
[135] *Université de Lyon, Université Lyon 1, CNRS/IN2P3, IPN-Lyon, Villeurbanne, Lyon, France*
[136] *Université de Strasbourg, CNRS, IPHC UMR 7178, F-67000 Strasbourg, France*
[137] *Université Paris-Saclay Centre d'Etudes de Saclay (CEA), IRFU, Départent de Physique Nucléaire (DPhN), Saclay, France*
[138] *Università degli Studi di Foggia, Foggia, Italy*
[139] *Università degli Studi di Pavia, Pavia, Italy*
[140] *Università di Brescia, Brescia, Italy*
[141] *Variable Energy Cyclotron Centre, Homi Bhabha National Institute, Kolkata, India*
[142] *Warsaw University of Technology, Warsaw, Poland*
[143] *Wayne State University, Detroit, MI, United States*
[144] *Westfälische Wilhelms-Universität Münster, Institut für Kernphysik, Münster, Germany*
[145] *Wigner Research Centre for Physics, Hungarian Academy of Sciences, Budapest, Hungary*
[146] *Yale University, New Haven, CT, United States*
[147] *Yonsei University, Seoul, Republic of Korea*

[i] Deceased.
[ii] Dipartimento DET del Politecnico di Torino, Turin, Italy.
[iii] M.V. Lomonosov Moscow State University, D.V. Skobeltsyn Institute of Nuclear, Physics, Moscow, Russia.
[iv] Department of Applied Physics, Aligarh Muslim University, Aligarh, India.
[v] Institute of Theoretical Physics, University of Wroclaw, Poland.